Spectroscopic Studies of DNA and ATP Binding to Human Polynucleotide Kinase: Evidence for a Ternary Complex†

Rajam S. Mani,* Feridoun Karimi-Busheri, Mesfin Fanta, Carol E. Cass, and Michael Weinfeld*

Department of Experimental Oncology, Cross Cancer Institute, and Department of Oncology, University of Alberta, Edmonton, Alberta T6G 1Z2, Canada

Received May 22, 2003

ABSTRACT: Human polynucleotide kinase (hPNK), which possesses both 5′-DNA kinase and 3′-DNA phosphatase activities, is a DNA repair enzyme required for processing and rejoining of single- and double-strand-break termini. Full-length hPNK was subjected to sedimentation and spectroscopic analyses in association with its ligands, a 20-mer oligonucleotide, ATP, and AMP-PNP (a nonhydrolyzable analogue of ATP). Sedimentation equilibrium measurements indicated that hPNK was a monomer in the presence and absence of the ligands. Circular dichroism measurements revealed that the ligands induced different conformational changes in hPNK, although AMP-PNP induced the same conformational changes as ATP. CD also indicated that the oligonucleotide could bind to the protein-AMP-PNP complex. Protein−ligand binding affinities and stoichiometries were determined by measuring changes in protein intrinsic fluorescence. Titrating hPNK with the oligonucleotide indicated tight binding with a K_d value of 1.3 μM and with 1:1 stoichiometry. A 5′-phosphorylated oligonucleotide with the same sequence exhibited an almost 6-fold lower affinity (K_d value, 7.2 μM). ATP and AMP-PNP bound with high affinity (K_d values, respectively, of 1.4 and 1.6 μM), and the observed binding stoichiometries were 1:1. Furthermore, the nonphosphorylated oligonucleotide was able to bind to hPNK in the presence of AMP-PNP with a K_d value of 2.5 μM, confirming the formation of a ternary complex. This study provides the first direct physical evidence for such a ternary complex involving a polynucleotide kinase, AMP-PNP, and an oligonucleotide, and supports a reaction mechanism in which ATP and DNA bind simultaneously to the enzyme.

Eukaryotic polynucleotide kinase/phosphatase (PNK) is a bifunctional enzyme that can phosphorylate 5′-OH termini and dephosphorylate 3′-phosphate termini of DNA (*1*, *2*). It is considered to be a putative DNA repair enzyme involved in the processing of strand-break termini to a form suitable for other proteins to complete the replacement of missing nucleotides and strand rejoining (*3*, *4*). A variety of genotoxic agents, including ionizing radiation, antitumor antibiotics such as bleomycin, and topoisomerase inhibitors such as camptothecin, generate strand-break termini that cannot be directly acted upon by DNA polymerases and ligases because these enzymes require 3′-OH and 5′-phosphate termini (*5*−*7*). Strand breaks produced by the AP lyase activities of DNA glycosylases require similar processing (*8*). Recent evidence from in vitro experiments indicates that PNK participates in single-strand-break repair (*4*, *9*) and nonhomologous end joining of double-strand breaks (*10*, *11*). A fission yeast knock-out mutant of the gene encoding Pnk1, the polynucleotide kinase of *Schizosaccharomyces pombe*, displays a pronounced hypersensitivity to ionizing radiation and camptothecin (*12*).

The cDNA for human PNK (hPNK) has been cloned and sequenced and shown to encode a 57.1-kDa polypeptide (*13*, *14*). Included among its identifiable domains are a Walker A box for binding ATP, which is the phosphate donor for the kinase activity, a phosphatase-associated domain (*15*), and a putative phosphopeptide binding forkhead-associated domain (*16*−*18*). The sequences of the ATP-binding and phosphatase-associated domains are highly conserved in all of the polynucleotide kinases sequenced to date, including those expressed by mammals, *S. pombe*, maize, and the T4 phage (*12*, *14*, *19*, *20*).

There are, however, several major differences, both biological and structural, between the mammalian and the T4-phage enzymes. Whereas the mammalian protein is considered to be a DNA repair enzyme, the phage enzyme acts on cleaved tRNA (*21*). The phage enzyme can phosphorylate DNA, RNA, oligonucleotides, and 3′-mononucleotides (*22*, *23*). In contrast, the kinase activity of the mammalian enzyme appears to be specific for DNA, with optimal activity on oligonucleotides of at least 20−30 nucleotides and no activity on oligonucleotides of ≤8 nucleotides (*3*, *24*). We recently determined that *N*-terminal

† This work was supported by the Canadian Institutes of Health Research, the Alberta Cancer Board, Alberta Cancer Foundation, the Alberta Heritage Foundation for Medical Research, and the National Cancer Institute of Canada. C.E.C. is Canada Research Chair in Oncology.

* To whom correspondence should be addressed. E-mail: rajam.mani@cancerboard.ab.ca and michaelw@cancerboard.ab.ca.

[1] Abbreviations: AMP-PNP, β,γ-imidoadenosine 5′-triphosphate; CD, circular dichroism; cDNA, complementary DNA.; EDTA, ethylenediaminetetraacetic acid; Gdn-HCl, guanidine hydrochloride; HEPES, *N*-(2-hydroxyethyl)piperazine; PCR, polymerase chain reaction; PMSF, phenylmethanesulfonyl fluoride; PNK, polynucleotide kinase; SDS, sodium dodecyl sulfate.

10.1021/bi030127b CCC: $25.00
Published on Web 09/26/2003

his-tagged hPNK is monomeric (*25*) and thus differs from T4 polynucleotide kinase, which in its active form is a homotetramer (*26*−*28*). On the basis of kinetic and structural studies, the T4 enzyme is believed to bind DNA and ATP simultaneously (*28*−*30*). However, there is only limited information regarding the mechanism of action of eukaryotic kinases.

We have shown previously that the binding of ATP perturbs the structure of hPNK, reducing the α-helical content (*25*). In the present study, the interaction between recombinant hPNK and an oligonucleotide with 20 residues was investigated by employing circular dichroism and intrinsic fluorescence measurements. The hPNK−ligand interactions resulted in partial quenching of fluorescence, and hence by carrying out fluorescence titrations with ATP (or AMP-PNP) and the oligonucleotide, we established the stoichiometries and the affinities with which these substrates were bound by hPNK. Our results indicated that hPNK bound both ATP and the oligonucleotide with a high affinity and induced conformational changes that affected both secondary and tertiary structures. Furthermore, we have demonstrated the formation of a ternary complex of hPNK, AMP-PNP, and an oligonucleotide, thus providing evidence supporting a sequential reaction mechanism.

EXPERIMENTAL PROCEDURES

Purification of Recombinant hPNK. The full-length hPNK cDNA was amplified by PCR using *Pfu* DNA polymerase and primers with tails that provided cleavage sites for *NcoI* (5′-TTTGAATTCCCCATGGGCGAGGTGGAGCCCCCG-GGC-3′) and *BamHI* (5′-CGCGGATCCTCAGCCCTCG-GAGAACTGGCAG-3′) and then subcloned into the expression plasmid pET-16b (Novagen, Madison, WI). Cloning the cDNA between the *NcoI* and *BamHI* sites leads to the production of an untagged protein. The modified plasmid was transfected into host *E. coli* bacterial strain BL21-CodonPlus (Stratagene, La Jolla, CA). The bacteria were grown at 37 °C in 4 L of LB medium containing ampicillin (50 μg/mL) and kanamycin (30 μg/mL) to an OD_{600} of 0.6, and protein expression was then induced by overnight incubation at room temperature in the presence of 100 μM isopropyl-1-thio-β-D-galactopyranoside (Sigma, St. Louis, MO).

Cells were harvested by centrifugation at 5000*g* at 4 °C for 30 min and resuspended in 50 mL of lysis buffer (150 mM NaCl, 50 mM Tris-HCl, pH 8.0, 1 mM EDTA, 0.1% β-mercapthoethanol, and 0.5 mM phenylmethylsulfonyl fluoride (PMSF)) containing a final concentration of 0.5 mg/mL lysozyme and 1% Triton-X 100. The suspension was stirred on ice for 30 min at 30 °C, and the bacteria were disrupted by sonication. The soluble fraction was separated from the insoluble fraction by centrifugation at 15 000*g* for 30 min at 4 °C. The salt concentration of the soluble fraction was raised to 500 mM, and polyethylenimine was added dropwise to a final concentration of 0.3% while stirring on ice. The sample was stirred on ice for another 20 min and then centrifuged at 15 000*g* for 20 min. Protein in the supernatant was precipitated by 50% ammonium sulfate (final concentration), followed by centrifugation at 15 000*g* for 30 min. The pellet was first resuspended in 40 mL of buffer A (50 mM Tris-HCl, pH 8.00, 1 mM EDTA, 0.1% β-mercapthoethanol, and 0.5 mM PMSF), and then the salt concentration was increased to 1.5 M by adding an additional 80 mL of buffer A containing 30.4 g of ammonium sulfate. The solution was loaded onto a 10-mL HiPrep 16/10 Butyl FF column (Amersham Pharmacia BioTech, Baie d'Urfe, PQ) equilibrated with buffer A plus 1.5 M ammonium sulfate. The protein was eluted with a 150-mL linear gradient of 1.5−0.0 M ammonium sulfate collected in 30 5-mL fractions. Fractions containing the highest concentration of PNK were pooled, and the buffer exchanged with buffer B (50 mM HEPES, pH 7.0, 0.1% β-mercapthoethanol, 1 mM EDTA and 0.5 mM PMSF) using a 30-kDa cutoff Ultrafree concentrator (Millipore, Bedford, MA). The sample was then applied to a 5-mL SP Sepharose Fast Flow cation-exchange column (Amersham Pharmacia BioTech). The column was washed with 20 mL of buffer A, and the enzyme was eluted with a 50-mL linear gradient of buffer B containing 0.0−1.0 M NaCl. Fractions containing PNK activity eluted between 0.4 and 0.5 M NaCl. The active fractions were pooled and concentrated using a 30-kDa cutoff Millipore ultrafree concentrator while exchanging the buffer content with buffer C (50 mM Tris-HCl, pH 8.0, 150 mM NaCl, 1 mM dithiothreitol, and 0.5 mM PMSF). The sample was applied on a HiLoad 16/60 Superdex 75 gel filtration column (Amersham Pharmacia BioTech), and purified protein was eluted with buffer C at a flow rate of 0.5 mL/min and collected in 2-mL fractions. For longer-term storage of the active fractions, aminoethylbenzenesulfonyl fluoride (Sigma) was added to a final concentration of 0.5 mM.

The protein purity was assessed using 10% SDS polyacrylamide gel electrophoresis. The purified protein possessed both 3′-phosphatase and 5′-kinase activities measured as previously described (*14*). The final protein concentration was adjusted to the desired level using a 30-kDa cutoff Millipore ultrafree concentrator while exchanging the buffer content with buffer D (50 mM Tris-HCl, pH 7.5, 100 mM NaCl, 5 mM $MgCl_2$, and 1 mM dithiothreitol). Protein concentrations were determined using an extinction coefficient, $\epsilon^{1\%}_{280nm,}$ of 12.2 (*25*).

Substrates. The oligonucleotide substrates, 5′-phosphorylated and nonphosphorylated, 5′-ATTACGAATGCCCA-CACCGC-3′, were synthesized by UCDNA Services (University of Calgary, Calgary, AB). AMP-PNP and ATP were purchased from Sigma (St. Louis, MO).

Sedimentation Equilibrium Studies. Sedimentation equilibrium experiments were carried out at 5 °C using interference optics. Prior to ultracentrifugation, protein samples were dialyzed for 48 h in 50 mM Tris-HCl buffer (pH 7.5), 100 mM NaCl, 5 mM $MgCl_2$, and 1 mM DTT. Samples (110 μL) were loaded into six-sector charcoal-filled Epon cells, allowing two concentrations of sample to be run simultaneously. Runs were performed at 12 000, 16 000, and 20 000 rpm, and each speed was maintained until there was no significant difference in scans taken 2 h apart to ensure that equilibrium was achieved. The sedimentation equilibrium data were evaluated with the Nonlin analysis program using a nonlinear least-squares curve-fitting algorithm (*31*). The program Sednterp (Sedimentation Interpretation Program, version 1.01) was employed to calculate the partial specific volume of the protein from the amino acid composition using the method of Cohn and Edsall (*32*).

Circular Dichroism Spectroscopy. Circular dichroism (CD) measurements were performed in a JASCO J-720 spectropolarimeter (Jasco, Easton, MD) calibrated with a 0.06% solution of ammonium *d*-camphor-10-sulfonate. The temperature in the sample chamber was maintained using a Lauda RM6 low-temperature circulator. Each sample was scanned 10 times, noise reduction was applied, and baseline buffer spectra were subtracted from sample spectra before calculating molar ellipticities. To obtain spectra in the far-UV region, the cell path length was 0.02 cm, and the protein concentration was 0.5 mg/mL. To obtain aromatic CD spectra, the cell path length was 1 cm, and the protein concentration was 1 mg/mL. The CD spectra were analyzed for secondary structure elements by the Contin ridge regression analysis program of Provencher and Glöckner (*33*).

Fluorescence Studies. Steady-state fluorescence spectra were measured at room temperature on a Perkin-Elmer LS-55 spectrofluorometer (with 5-nm spectral resolution for excitation and emission) using 0.2−0.4 μM solutions of purified recombinant hPNK. Protein fluorescence was excited at 295 nm, and fluorescence emission spectra were recorded in the 300−400-nm range; changes in fluorescence were usually monitored at the emission maximum (344 nm). In studying the effects of ligands on protein fluorescence intensities, additions to hPNK samples were made from ligand stock solutions, keeping the dilution below 3%, and fluorescence intensities were corrected for dilution factors. Background quenching, if present (<2%), was eliminated by subtracting the signal obtained from a buffer solution that contained the appropriate quantity of ligand. The total absorption of the enzyme samples was kept below 0.08 at 295 nm.

Analysis of Enzyme Fluorescence Quenching Data. The analysis of fluorescence quenching data took into account three types of quenching mechanisms: dynamic quenching due to time-dependent diffusive collisions between the fluorophore and quencher; static quenching as a result of the formation of a nonfluorescent ground-state complex between the fluorophore and quencher; and combined dynamic and/or static quenching of fluorophores differing in accessibility to the quencher. Fluorescence quenching data are most often described in terms of the Stern−Volmer equation:

$$\frac{F_0}{F} = 1 + K_{SV}[Q] = \frac{\tau_0}{\tau} \qquad (1)$$

where τ_0 and τ are the fluorescence lifetimes, respectively, in the absence and presence of quencher (Q) and F_0 and F represent the fluorescence intensities at the emission maximum in the absence and presence of Q, respectively. K_{SV} is the Stern−Volmer constant for collisional quenching and may be obtained from the slope of a linear plot of F_0/F versus [Q] for a homogeneous population of emitting fluorophores when they are equally accessible to the quenching ligand. However, in proteins containing multiple tryptophans, if some of the tryptophan residues are buried and thus not accessible to quencher, then the Stern−Volmer plot will deviate from linearity toward the *x* axis. When two fluorophore populations are present and one is not accessible to quencher, a modified form of the Stern−Volmer equation is required to analyze the quenching of heterogeneous emitting fluorophores (*34*, *35*):

$$\frac{F_0}{(F_0 - F)} = \frac{1}{([Q]f_a K_{SV})} + \frac{1}{f_a} \qquad (2)$$

where f_a is the fractional accessibility [i.e., the maximum fraction of the protein fluorescence (tryptophan residues) accessible to Q]. A plot of $F_0/(F_0 - F)$ versus 1/[Q] should yield a straight line having a slope of $1/f_a K_{SV}$ and an intercept of $1/f_a$.

RESULTS

Expression and Purification of hPNK. Active recombinant hPNK was produced in *E. coli* and purified by sequential chromatography on hydrophobic, cation-exchange, and gel filtration columns. The SDS gel, stained with Coomassie blue, indicated purification to near-homogeneity (Figure 1A). The relative molecular mass (M_r) of 58 000 agreed with the value of 57 102 calculated for the amino acid sequence predicted from the cDNA encoding hPNK. The UV absorption spectrum of hPNK revealed an absorption maximum at 280 nm, characteristic of tyrosine residues, and a shoulder around 290 nm, characteristic of tryptophan residues. The $^{280}/_{260}$ and $^{280}/_{290}$ absorbance ratios were 1.60 and 1.33, respectively. Protein concentrations were determined using an extinction coefficient, $\epsilon^{1\%}_{280nm}$, of 12.2, a value that was established by the refractometric method of Babul and Stellwagen (*36*). The purified recombinant protein exhibited both kinase and phosphatase activities (*14*).

Sedimentation Equilibrium Studies. Sedimentation equilibrium results and nonlinear regression fits were obtained at three different speeds for two initial loading concentrations of 0.25 mg/mL (4.3 μM) and 0.5 mg/mL (8.6 μM) for hPNK (Figure 1B and C). The sedimentation equilibrium data fit well to a single-species model with no evidence of aggregation, and a calculated M_r of 58 500 is consistent with the value of 58 000 obtained by SDS polyacrylamide gel electrophoresis. The absence of aggregation, which implies that hPNK was monomeric, agreed with our previous results obtained with recombinant his-tagged hPNK (*25*). The M_r obtained in the presence of 10 μM oligonucleotide was 59 500 (data not shown), suggesting that hPNK did not undergo any aggregation in the presence of the oligonucleotide.

Circular Dichroism Studies. Information concerning the secondary structure of hPNK was obtained from far-UV CD data, and a typical far-UV CD spectrum of hPNK is shown in Figure 2A. hPNK exhibited two large, negative CD bands centered at 218 and 209 nm, indicating the presence of α-helical organization. The observed molar ellipticities, $[\theta]_M$, at these two wavelengths were -7100 ± 200 and -8100 ± 200 deg cm^2 dmol^{-1}, respectively. The CD spectra were analyzed for secondary structural elements by the Contin ridge regression analysis program (*33*). The protein possessed 23% α-helix and 60% β-sheet−β-turn, and the remaining 17% represented random structure (Table 1).

It is evident from the results of Figure 2A that the addition of oligonucleotide induced a conformational change in hPNK because the molar ellipticity values $[\theta]_M$ at 218 and 209 nm were reduced to -6400 ± 200 and -7100 ± 200 deg cm^2 dmol^{-1}, respectively, with significant changes in secondary

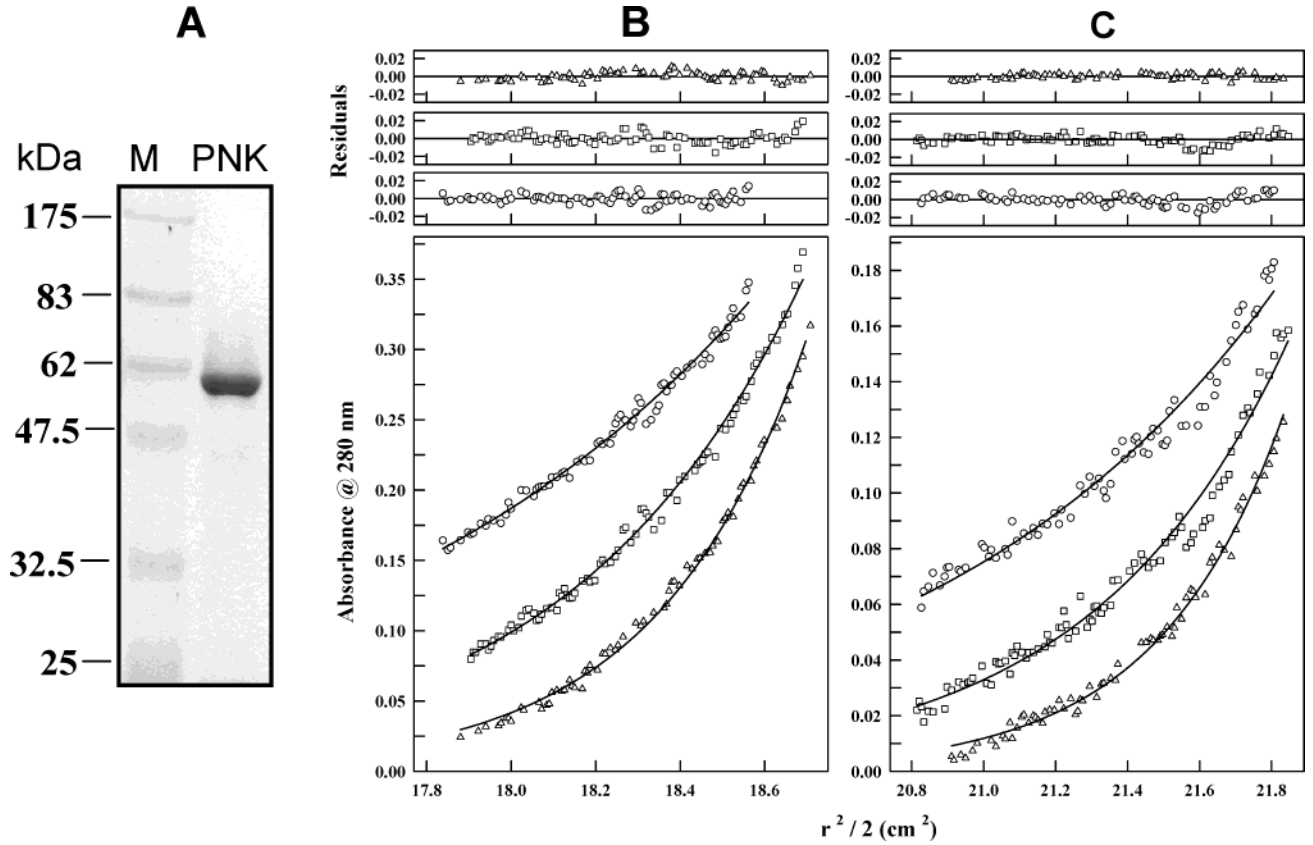

FIGURE 1: (A) Electrophoresis of purified hPNK in a 10% SDS polyacrylamide gel. The left lane shows the size markers with sizes marked in kDa. (B) Sedimentation equilibrium profiles at 12 000 (○), 16 000 (□), and 20 000 (△) at 5 °C for 48 h. The absorbance as a function of radial position for hPNK is shown for two initial loading concentrations: (B) 0.25 mg/mL and (C) 0.5 mg/mL. Global nonlinear regression fitting (solid lines) of all six data sets was performed for a single-component system. The residuals for each fit are shown in the upper panels.

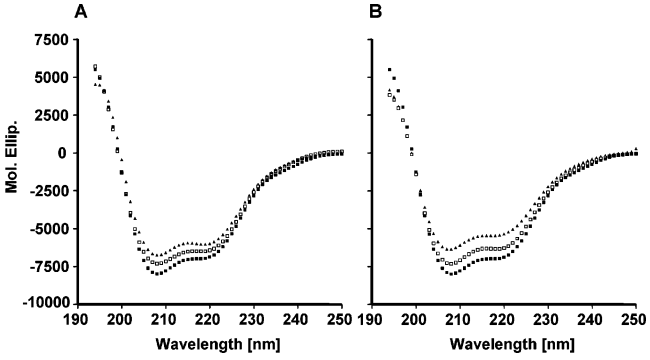

FIGURE 2: (A) Far-UV−CD spectrum of hPNK (■), hPNK + 10 μM ATP (▲), and hPNK + 10 μM oligonucleotide (□). (B) Far-UV−CD spectrum of hPNK (■), hPNK + 10 μM AMP-PNP (▲), and hPNK + 10 μM AMP-PNP + 10 μM oligonucleotide (□). The concentration of hPNK was 0.55 mg/mL in 50 mM Tris, pH 7.5, 100 mM NaCl, 5 mM $MgCl_2$, and 1 mM DTT.

structure resulting in a loss of α-helical content (Table 1). The binding of ATP (Figure 2A) also altered the CD spectrum of hPNK. The binding of AMP-PNP, a nonhydrolyzable analogue of ATP, which is an inhibitor of kinases (*30*), produced changes similar to ATP in the CD spectrum of hPNK (Figure 2B, Table 1).

The ability of hPNK to bind oligonucleotide in the presence of AMP-PNP is shown in Figure 2B. For this experiment, AMP-PNP was first added to hPNK (1:1 mole ratio), and the resulting CD spectrum was compared to the CD spectrum generated following the addition of the oligonucleotide (oligonucleotide to protein molar ratio was 1:1) to the binary complex. The ellipticity values at 218 and 209 nm in the absence and presence of oligonucleotide were −5600 ± 200 and −6300 ± 200 and −6300 ± 200 and −7200 ± 200 deg cm^2 $dmol^{-1}$, respectively. These results demonstrated that the binding of oligonucleotide by hPNK in the presence of AMP-PNP altered the secondary structure of the binary complex.

Table 1: Effects of Ligands on the Secondary Structure of HPNK[a]

sample	α-helix (%)	β-sheet (%)[b]	β-turn (%)[b]	random (%)[b]
hPNK	23	41	19	17
hPNK + ATP	15	44	23	18
hPNK + AMP-PNP	14	44	24	18
hPNK + oligo	16	46	21	17
hPNK + AMP-PNP + oligo	18	42	22	18

[a] The concentration of ligand used was 10 μM, and the protein-to-ligand molar ratio was 1:1. The CD spectra were analyzed by the Contin ridge regression analysis program of Provencher-Glöckner (*33*). [b] Although the calculations suggest a concomitant increase in β structure with the loss of α-helical structure, it must be borne in mind that CD analysis yields close agreement with X-ray data only for α-helical structure (r^2 = 0.96), and less confidence should be placed in the estimation of the non-α-helical structures (r^2 = 0.94 for the β sheet, 0.31 for the β turn, and 0.49 for random structure) (*33*).

Near-UV CD Spectra. Near-UV (250−320 nm) CD spectroscopy provides information on the environment of aromatic residues in folded proteins. The aromatic CD spectrum of hPNK in the absence and presence of the oligonucleotide is shown in Figure 3. The ellipticity of the protein was positive between 250 and 300 nm. The CD band

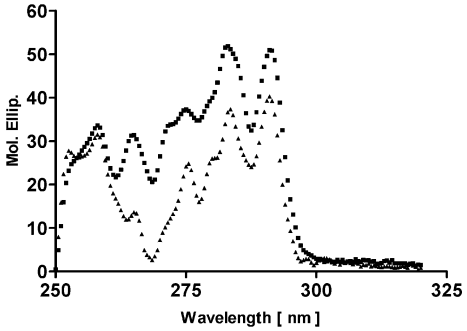

FIGURE 3: Aromatic CD spectra of hPNK (1 mg/mL) in 50 mM Tris, pH 7.5, 100 mM NaCl, 5 mM $MgCl_2$, and 1 mM DTT alone (■) or with 2 μM oligonucleotide (▲).

at 291 nm was due to tryptophan residues, the bands at 283 and 279, to tyrosine residues, and the two bands at 268 and 262, to phenylalanine residues. Adding the oligonucleotide perturbed the aromatic residues. The ellipticity value for the CD bands at 291, 287, and 279 nm decreased, indicating perturbations of tryptophan, tyrosine, and phenylalanine residues. Although the binding of ATP also perturbed the environments of these aromatic residues (*25*), the ellipticity values at the CD bands corresponding to tryptophan and tyrosine residues increased rather than decreased, indicating that ATP and the oligonucleotide induced different conformational changes in hPNK.

Fluorescence Spectroscopy. Although hPNK has nine tryptophan and nine tyrosine residues, the observed fluorescence was due to tryptophan residues because the protein was excited at 295 nm. Fluorescence spectra of hPNK were measured in Tris buffer, pH 7.5, in the absence and presence of 6 M guanidine hydrochloride (Gdn-HCl). In the absence of the denaturant, the emission maximum was at 344 ± 1 nm, and in 6 M Gdn-HCl, the emission maximum was red shifted to 353 ± 1 nm and was accompanied by a decrease in fluorescence intensity. These results indicated that the unfolding of hPNK in 6 M Gdn-HCl exposed the partly buried tryptophan residues to a more polar environment.

We studied the effects of the binding of substrates (ATP or the oligonucleotide) and the inhibitor (AMP-PNP) to hPNK by determining the response of its fluorescence to increasing concentrations of ligand. The hPNK−ligand interaction was accompanied by a partial quenching of fluorescence with no change in the emission maximum, which enabled the determination of the binding affinity (K_d) and stoichiometry by following fluorescence quenching (a measure of ligand binding) as a function of ligand concentration. A plot of the relative fluorescence intensity versus the concentration of ATP is shown as an inset in Figure 4A. The maximum quenching of fluorescence intensity observed at saturating concentrations of ATP was taken as 1, and the observed quenching at different concentrations of ATP was plotted as the fraction of bound versus free ATP concentration (Figure 4A). Nonlinear regression analysis of the binding data revealed unimodal binding with a K_d value of 1.4 ± 0.2 μM. In Figure 4B, $\log(F_0 - F)/(F - F_\infty)$ is plotted against log [ATP], where F_0, F, and F_∞ are the fluorescence intensities of solutions of enzyme alone, enzyme in the presence of various concentrations of ATP, and enzyme saturated with ATP, respectively. This plot yielded a slope of 1.04, indicating a 1:1 interaction between ATP and hPNK.

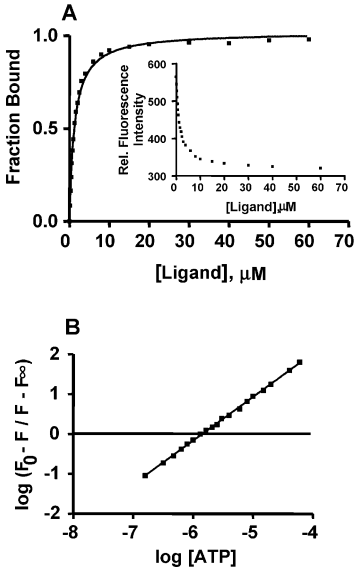

FIGURE 4: Fluorescence titration of hPNK vs ATP. (A) hPNK (0.4 μM) against ATP in 50 mM Tris, pH 7.5, 100 mM NaCl, 5 mM $MgCl_2$, and 1 mM DTT. The protein was excited at 295 nm, and the fluorescence intensity was monitored at 344 nm (see inset). Fraction of bound (i.e., relative fluorescence quenching) versus free ATP concentration is plotted. (B) Sample plot of fluorescence data from titration with ATP. F_0, F, and F_∞ are the relative fluorescence intensities at 344 nm of hPNK alone, hPNK in the presence of a given concentration of ATP, and hPNK saturated with ATP, respectively. The plot is according to Chipman et al. (*42*).

When similar studies were conducted with AMP-PNP (data not shown), hPNK bound AMP-PNP with a high affinity, with a K_d value of 1.6 ± 0.2 μM and a binding ratio of 1:1.

We also studied the binding of the nonphosphorylated and 5′-phosphorylated 20-mer oligonucleotides to hPNK. The nonphosphorylated oligonucleotide, a substrate for the kinase activity of PNK, was bound with high affinity (K_d value, 1.3 μM), and because the value of the slope for the logarithmic plot was 1.04, this indicates 1:1 stoichiometry (Figure 5A and B). However, the 5′-phosphorylated oligonucleotide, which can be considered to be a product of the enzymatic reaction of PNK, showed markedly lower affinity for PNK with a K_d value of 7.2 μM, and the value of the slope for the logarithmic plot was 0.92, indicating 1:1 stoichiometry (Figure 5C and D). The difference in affinities for the two forms of the oligonucleotide demonstrate that the enzyme can differentiate between phosphorylated and nonphosphorylated DNA termini.

The binding of the nonphosphorylated oligonucleotide to hPNK in the presence of 10 μM AMP-PNP is shown in Figure 6A and B. At this concentration of AMP-PNP, all of the hPNK should exist as a binary complex with AMP-PNP because the K_d value for AMP-PNP is 1.6 μM. The observed fluorescence emission intensity of this binary complex was taken as the control value in the absence of the oligonucleotide. Quenching of the fluorescence emission intensity was then monitored as a function of the concentration of added oligonucleotide to determine the binding affinity of the oligonucleotide to the binary complex. The affinity of hPNK for the oligonucleotide was not significantly affected by the presence of AMP-PNP (K_d value was 2.5 ± 0.3 μM), suggesting the formation of a ternary complex between hPNK, AMP-PNP, and the oligonucleotide. The plot of $\log(F_0 - F)/(F - F_\infty)$ versus log[oligonucleotide] was linear

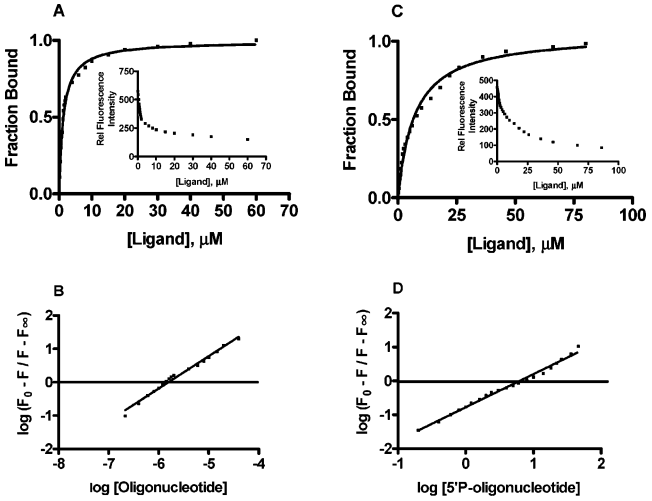

FIGURE 5: Fluorescence titration of hPNK vs oligonucleotide. (A) hPNK (0.4 μM) against oligonucleotide in 50 mM Tris, pH 7.5, 100 mM NaCl, 5 mM $MgCl_2$, and 1 mM DTT. The protein was excited at 295 nm, and the fluorescence intensity at 344 nm was monitored (see inset). Fraction of bound (i.e., relative fluorescence quenching) versus free oligonucleotide concentration is plotted. (B) Sample plot of fluorescence data from titration with oligonucleotide, according to Chipman et al. (*42*). (C) hPNK (0.4 μM) against 5′-phosphorylated oligonucleotide. (D) Sample plot of fluorescence data from titration with 5′-phosphorylated oligonucleotide.

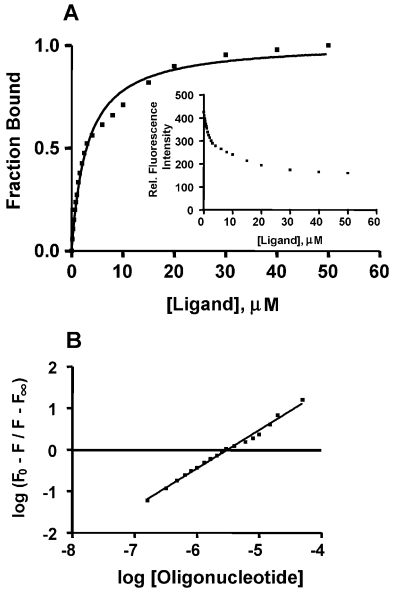

FIGURE 6: Fluorescence titration of hPNK and AMP-PNP vs oligonucleotide. (A) hPNK (0.4 μM) + 10 μM AMP-PNP against oligonucleotide in 50 mM Tris, pH 7.5, 100 mM NaCl, 5 mM $MgCl_2$, and 1 mM DTT. The protein was excited at 295 nm, and the fluorescence intensity at 344 nm was monitored (see inset). Fraction of bound (i.e., relative fluorescence quenching) versus free oligonucleotide concentration is plotted. (B) Sample plot of fluorescence data from titration with oligonucleotide, according to Chipman et al. (*42*).

(slope was 0.94), indicating that the hPNK/AMP-PNP complex bound the oligonucleotide with 1:1 stoichiometry.

Enzyme Fluorescence Quenching by Ligands. Increasing the concentration of the ligands led to the decreased fluorescence of hPNK with no change in the emission maximum. The Stern−Volmer plot for fluorescence quenching by ATP is shown in Figure 7. As seen in the inset, the plot of F_0/F versus [Q] was not linear, and the observed downward curvature indicated the presence of inaccessible

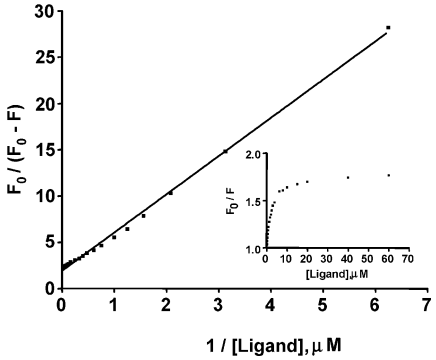

FIGURE 7: Modified Stern−Volmer plot of the steady-state quenching of hPNK fluorescence by ATP. The decrease in fluorescence ($F - F_0$) at 295-nm excitation and 344-nm emission is expressed as a function of the reciprocal concentration of ATP. F and F_0 are the relative fluorescence intensities at 344 nm of hPNK alone or in the presence of a given concentration of ATP, respectively. The inset represents the ratio of F_0/F vs the ATP concentration.

Table 2: Stern−Volmer Constants (K_{SV}, f_a) Obtained from Fits of the Modified Stern−Volmer Equation to Protein Fluorescence[a]

ligand	K_{SV} (μM^{-1})	f_a
ATP	0.68	0.45
AMP-PNP	0.55	0.50
oligo	0.70	0.72
5′P-oligo	0.40	0.36
AMP-PNP + oligo	0.45	0.62

[a] Stern−Volmer constants (K_{SV}, μM^{-1}) and the fractional accessibility (f_a) were determined from the slope and the intercept on the y axis, as described in Experimental Procedures.

tryptophans. This result indicated that fluorescence quenching was not due to a single class of fluorophores, and the modified form of the Stern−Volmer equation for heterogeneous emitting fluorophores was applied. Replotting of the data yielded a straight line. The intercept on the y axis (f_a^{-1}) was 2.2, indicating that 45% of the protein fluorescence (tryptophan residues) was accessible to quencher (ATP). The Stern−Volmer quenching constant (K_{SV}) of the accessible fraction of tryptophan residue(s) was 0.68. The values of f_a and K_{SV} obtained with AMP-PNP and the oligonucleotide are given in Table 2. The accessibility of tryptophan residues (f_a) to these quenchers was oligonucleotide > oligonucleotide + AMP-PNP > AMP-PNP > ATP > 5′-phosphorylated oligonucleotide. The values of the Stern−Volmer quenching constant, which corresponds to the association constant for enzyme−ligand complexes (*37*), decreased in the following order: oligonucleotide > ATP > AMP-PNP > oligonucleotide + AMP-PNP > 5′-phosphorylated oligonucleotide. The rank order was in agreement with that of the K_d values obtained from the analysis of fluorescence titrations.

DISCUSSION

hPNK is a DNA repair enzyme required for the processing and rejoining of single- and double-strand-break termini. The complete cDNA, which encodes a 521 amino acid protein (57.1 kDa), was expressed in *E. coli*, and the purified recombinant protein exhibited both kinase and phosphatase activities. In an earlier study, we demonstrated that *N*-terminal his-tagged hPNK exists as a monomer in solution (*25*). In this study, we observed that wild-type hPNK also

exists as a monomer in solution, indicating that the modification of the *N* terminus has no effect on the oligomeric structure of the protein. More importantly, the binding of a 20-mer oligonucleotide has no significant effect on the sedimentation characteristics of hPNK, indicating that protein remains monomeric when bound to its substrate.

It is instructive to compare the properties of hPNK to those of T4-phage PNK, a polynucleotide kinase for which detailed biophysical data and the 3-D crystal structure have been obtained (*27*, *28*). Even though both hPNK and T4 PNK are bifunctional enzymes with 5′-kinase and 3′-phosphatase activities, they exhibit different substrate specificities (*38*). The human and T4 enzymes differ structurally in that T4 PNK in its active form is a 140-kDa homotetramer whereas hPNK is a 60-kDa monomer. The secondary structure of hPNK also differs significantly from that of T4 PNK in that the T4 enzyme has ∼45% α-helix and ∼25% β structure (*26*) whereas hPNK has ∼25% α-helix and ∼50% β structure (*25*) and the kinase and phosphatase domains in hPNK are reversed compared to those in T4 PNK (*12*−*14*). The substantial structural differences between hPNK and T4 PNK may explain some of the differences in their structure−function relationships. For example, the observed differences in substrate specificities can be rationalized on the basis of steric hindrance arising from the different sizes of the two active enzymes. In the present study, spectroscopic techniques have been employed to study the interaction of substrates with hPNK.

The effects of binding of ATP, AMP-PNP, and an oligonucleotide of 20 residues alone or in the presence of AMP-PNP on the intrinsic fluorescence of hPNK were measured to determine the binding affinities (K_d) and stoichiometries of these ligands. Fluorescence spectroscopy indicated that the binding of either ATP or AMP-PNP with a K_d value of 1.4 or 1.6 μM, respectively, induced a conformational change. A K_m value for ATP of 2 μM has been reported for the kinase activity of purified rat liver PNK (*24*), and T4 PNK also binds ATP with high affinity (K_d = 2 μM) (*30*). In this study, we have demonstrated for the first time that hPNK also binds an oligonucleotide substrate with high affinity (K_d = 1.3 μM) in a 1:1 stoichiometric manner. In an earlier kinetic study with purified calf thymus PNK (*3*), we obtained a K_m value of 1.7 μM with a 24-mer oligonucleotide, in excellent agreement with the spectroscopic findings of the current study. In the present study, we were also able to establish the stoichiometry. By comparison, the binding affinity of the 5′-phosphorylated oligonucleotide was almost 6-fold lower, indicating that binding is primarily dependent on the nature of the 5′-terminus, as would be expected from its enzymatic function. The Stern−Volmer constants obtained from fluorescence quenching analysis (Table 2) suggest that hPNK binding to the 5′-phosphorylated oligonucleotide differs structurally from the specific binding to the nonphosphorylated oligonucleotide.

Fluorescence and near-UV−CD data showed that binding to the nonphosphorylated oligonucleotide perturbed the aromatic residues (tryptophans, tyrosines, and phenylalanines). The proposed DNA-binding domain (*14*) is postulated to be in the C-terminal end (residues 402−464) of hPNK, a region that contains only one of the nine known tryptophans (W-402). In future studies, we will make use of site-directed mutagenesis to determine if this tryptophan becomes more exposed upon oligonucleotide binding to hPNK.

The ability of hPNK to bind the oligonucleotide with high affinity (K_d = 2.5 μM) in the presence of AMP-PNP with 1:1 (hPNK-AMP-PNP: oligonucleotide) stoichiometry (Figure 6B) demonstrated the formation of a ternary complex involving hPNK, AMP-PNP, and the oligonucleotide. The Stern−Volmer constants obtained from the fluorescence quenching data (Table 2) also clearly demonstrate the formation of a ternary complex with significantly different K_{SV} and f_a values than those of the binary complexes of hPNK-AMP-PNP and hPNK-oligonucleotide. This indicates that the binding of the oligonucleotide to the hPNK-AMP-PNP complex does not cause the release of AMP-PNP because the observed K_{SV} and f_a values do not correspond to the hPNK-oligonucleotide complex. In the repair of DNA strand breaks by hPNK, ATP is the phosphate donor and is required for the phosphorylation of the 5′-OH end (*39*). Because AMP-PNP is a nonhydrolyzable analogue of ATP, it was used to demonstrate the formation of the proposed ternary complex. The spectroscopic data indicated that AMP-PNP strongly mimicked ATP in its interaction with hPNK. Because the ATP concentration in cells is typically ∼2 mM, cellular hPNK will normally be saturated with ATP, and we therefore assessed the interaction of the oligonucleotide with hPNK in the presence of AMP-PNP. The fluorescence quenching results indicated that substrates (ATP and the oligonucleotide) induced different conformational changes in hPNK and therefore must have either perturbed the same tryptophan residue(s) differently or interacted with different tryptophan residues.

Phosphate transfer by a polynucleotide kinase could proceed by one of two possible mechanisms: (i) a ping-pong mechanism or (ii) a sequential mechanism (*29*). A ping-pong mechanism would entail the initial binding of ATP and the subsequent release of ADP (with retention by the enzyme of inorganic phosphate) before the enzyme binds the DNA. However, a sequential reaction mechanism implies that both ATP and DNA bind before either product dissociates. On the basis of the results of initial-rate studies at different substrate concentrations, product inhibition studies, and the reversible nature of the reaction, Lillehaug and Kleppe argued that T4 PNK activity proceeds according to a sequential reaction mechanism (*29*, *40*). Galburt et al. (*28*) have also proposed a ternary complex of T4 PNK bound to DNA and ATP on the basis of the strong homology between the kinase domain of T4 PNK and adenylate kinase and the structure of adenylate kinase with bound adenylate and AMP-PNP (*41*). Our finding that hPNK bound the oligonucleotide with high affinity in the presence of AMP-PNP demonstrated the formation of a ternary complex, thus providing direct physical evidence supporting the sequential reaction mechanism for polynucleotide kinases. However, the order of binding of the ligands could conceivably be a random process because the binding affinity for DNA was not influenced by the presence of AMP-PNP.

ACKNOWLEDGMENT

We thank Robert Luty for CD analysis, and Leslie D. Hicks for performing analytical ultracentrifugation experiments.

REFERENCES

1. Pheiffer, B. H., and Zimmerman, S. B. (1982) *Biochem. Biophys. Res. Commun. 109*, 1297−1302.
2. Habraken, Y., and Verly, W. G. (1983) *FEBS Lett. 160*, 46−50.
3. Karimi-Busheri, F., and Weinfeld, M. (1997) *J. Cell. Biochem. 64*, 258−272.
4. Karimi-Busheri, F., Lee, J., Tomkinson, A. E., and Weinfeld, M. (1998) *Nucleic Acids Res. 26*, 4395−4400.
5. Coquerelle, T., Bopp, A., Kessler, B., and Hagen, U. (1973) *Int. J. Radiat. Biol. Relat. Stud. Phys. Chem. Med. 24*, 397−404.
6. Povirk, L. F. (1996) *Mutat. Res. 355*, 71−89.
7. Li, T. K., and Liu, L. F. (2001) *Annu. Rev. Pharmacol. Toxicol. 41*, 53−77.
8. Hazra, T. K., Izumi, T., Kow, Y. W., and Mitra, S. (2003) *Carcinogenesis 24*, 155−157.
9. Whitehouse, C. J., Taylor, R. M., Thistlethwaite, A., Zhang, H., Karimi-Busheri, F., Lasko, D. D., Weinfeld, M., and Caldecott, K. W. (2001) *Cell 104*, 107−117.
10. Chappell, C., Hanakahi, L. A., Karimi-Busheri, F., Weinfeld, M., and West, S. C. (2002) *EMBO J. 21*, 2827−2832.
11. Inamdar, K. V., Pouliot, J. J., Zhou, T., Lees-Miller, S. P., Rasouli-Nia, A., and Povirk, L. F. (2002) *J. Biol. Chem. 277*, 27162−27168.
12. Meijer, M., Karimi-Busheri, F., Huang, T. Y., Weinfeld, M., and Young, D. (2002) *J. Biol. Chem. 277*, 4050−4055.
13. Jilani, A., Ramotar, D., Slack, C., Ong, C., Yang, X. M., Scherer, S. W., and Lasko, D. D. (1999) *J. Biol. Chem. 274*, 24176−24186.
14. Karimi-Busheri, F., Daly, G., Robins, P., Canas, B., Pappin, D. J., Sgouros, J., Miller, G. G., Fakhrai, H., Davis, E. M., Le Beau, M. M., and Weinfeld, M. (1999) *J. Biol. Chem. 274*, 24187−24194.
15. Jilani, A., Slack, C., Matheos, D., Zannis-Hadjopoulos, M., and Lasko, D. D. (1999) *J. Cell. Biochem. 73*, 188−203.
16. Durocher, D., Henckel, J., Fersht, A. R., and Jackson, S. P. (1999) *Mol. Cell 4*, 387−394.
17. Moreira, M. C., Barbot, C., Tachi, N., Kozuka, N., Uchida, E., Gibson, T., Mendonca, P., Costa, M., Barros, J., Yanagisawa, T., Watanabe, M., Ikeda, Y., Aoki, M., Nagata, T., Coutinho, P., Sequeiros, J., and Koenig, M. (2001) *Nat. Genet. 29*, 189−193.
18. Caldecott, K. W. (2003) *Cell 112*, 7−10.
19. Betti, M., Petrucco, S., Bolchi, A., Dieci, G., and Ottonello, S. (2001) *J. Biol. Chem. 276*, 18038−18045.
20. Midgley, C. A., and Murray, N. E. (1985) *EMBO J. 4*, 2695−2703.
21. Amitsur, M., Levitz, R., and Kaufmann, G. (1987) *EMBO J. 6*, 2499−2503.
22. Richardson, C. C. (1965) *Proc. Natl. Acad. Sci. U.S.A 54*, 158−165.
23. Novogrodsky, A., and Hurwitz, J. (1966) *J. Biol. Chem. 241*, 2923−2932.
24. Levin, C. J., and Zimmerman, S. B. (1976) *J. Biol. Chem. 251*, 1767−1774.
25. Mani, R. S., Karimi-Busheri, F., Cass, C. E., and Weinfeld, M. (2001) *Biochemistry 40*, 12967−12973.
26. Lillehaug, J. R. (1977) *Eur. J. Biochem. 73*, 499−506.
27. Wang, L. K., Lima, C. D., and Shuman, S. (2002) *EMBO J. 21*, 3873−3880.
28. Galburt, E. A., Pelletier, J., Wilson, G., and Stoddard, B. L. (2002) *Structure (Camb) 10*, 1249−1260.
29. Lillehaug, J. R., and Kleppe, K. (1975) *Biochemistry 14*, 1221−1225.
30. Kleppe, K., and Lillehaug, J. R. (1979) *Adv. Enzymol. Relat. Areas Mol. Biol. 48*, 245−275.
31. Johnson, M. L., Correia, J. J., Yphantis, D. A., and Halvorson, H. R. (1981) *Biophys. J. 36*, 575−588.
32. Cohn, E. J., and Edsall, J. T. (1943) in *Proteins* (Cohn, E. J., Edsall, J. T., Eds.) pp 370−381, Reinhold Publishing Corporation, New York.
33. Provencher, S. W., and Glockner, J. (1981) *Biochemistry 20*, 33−37.
34. Lehrer, S. S. (1971) *Biochemistry 10*, 3254−3263.
35. Lehrer, S. S., and Leavis, P. C. (1978) *Methods Enzymol. 49*, 222−236.
36. Babul, J., and Stellwagen, E. (1969) *Anal. Biochem. 28*, 216−221.
37. Lakowicz, J. R. (1983) *Principles of Fluorescence Spectroscopy*, Plenum Press, New York.
38. Caldecott, K. W. (2002) *Structure (Camb) 10*, 1151−1152.
39. Habraken, Y., and Verly, W. G. (1986) *Nucleic Acids Res. 14*, 8103−8110.
40. Cleland, W. W. (1963) *Biochim. Biophys. Acta 67*, 104−137.
41. Berry, M. B., Meador, B., Bilderback, T., Liang, P., Glaser, M., and Phillips, G. N., Jr. (1994) *Proteins 19*, 183−198.
42. Chipman, D. M., Grisaro, V., and Sharon, N. (1967) *J. Biol. Chem. 242*, 4388−4394.

BI030127B